^{1}H MAS, ^{15}N CPMAS, and DFT Investigation of Hydrogen-Bonded Supramolecular Adducts between the Diamine 1,4-Diazabicyclo-[2.2.2]octane and Dicarboxylic Acids of Variable Chain Length

Roberto Gobetto,*[,†] Carlo Nervi,[†] Enrico Valfrè,[†] Michele R. Chierotti,[†] Dario Braga,*[,‡] Lucia Maini,[‡] Fabrizia Grepioni,[§] Robin K. Harris,*[,||] and Phuong Y. Ghi[||]

Università di Torino, Via P. Giuria 7, 10125 Torino, Italy, Dipartimento di Chimica G. Ciamician, Università di Bologna, Via F. Selmi 2, 40126 Bologna, Italy, Dipartimento di Chimica, Università di Sassari, Via Vienna 2, 07100 Sassari, Italy, and Department of Chemistry, University of Durham, South Road, Durham, U.K., DH1 3LE

Received June 11, 2004. Revised Manuscript Received November 18, 2004

Supramolecular adducts of formula $[N(CH_2CH_2)_3N]-H-[OOC(CH_2)_nCOOH]$ ($n = 1-7$) have been obtained by mechanochemical reaction of solid dicarboxylic acids of variable chain length $HOOC(CH_2)_nCOOH$ ($n = 1-7$) with solid 1,4-diazabicyclo[2.2.2]octane (dabco). ^{1}H MAS and ^{15}N CPMAS spectra have been measured to investigate the presence of intermolecular hydrogen bonds between acid and base. Proton and nitrogen chemical shifts allow a distinction to be made between $N^{+}-H\cdots O^{-}$ interactions (with proton transfer) and $N\cdots H-O$ interactions (without proton transfer) and between strong and weak hydrogen bonds. Correlations among isotropic ^{1}H, ^{15}N chemical shift data and the N−O distances of the atoms involved in the hydrogen bond interaction are found. Density functional theory, applied to explore changes upon hydrogen bonding in the ^{1}H and ^{15}N shielding parameters, is in agreement with the experimental values found by solid-state NMR spectroscopy. Hydrogen/deuterium H/D isotope effects on the ^{15}N NMR chemical shifts have been also investigated.

1. Introduction

Hydrogen bonding (HB) is a phenomenon of paramount importance in chemistry and plays a unique role in nature. Both weak and strong HB have been investigated by physical and chemical methods[1,2] and it is well-known they contribute to the structures, physical properties, and chemical reactivity of molecules and molecular complexes. For example, molecular recognition of the nucleic acid duplex is based on the multiple weak HB formation.[3−7] Conversely, strong HBs such as low-barrier hydrogen bonds (LBHBs) or single-well hydrogen bonds (SWHBs) appear to be essential in all enzyme-catalyzed reactions, although why they are essential and how they promote reactions are open questions.[8] In the field of supramolecular chemistry, which has become one of the central topics in chemistry for the design of molecular systems,[9−13] the HB is the most important interaction because it combines directionality and strength with selectivity.[14,15] These peculiar behaviors make HB the preferred interaction in many crystal engineering studies, as demonstrated by the large number of papers devoted to the self-organization of organic molecules into one-, two-, or three-dimensional hydrogen-bonded architectures.[14,16−22] The energy of the weak HB is prevalently dominated by electrostatic factors, whereas strong hydrogen bonds are short in length and show magnetic and vibrational properties that are consistent with a covalent rather than electrostatic attraction. However, polarization, charge transfer, and exchange repulsion also play an important role. HB strengths can vary from 5 kJ mol^{-1} to hundreds of kJ mol^{-1} depending on the molecules

* Corresponding authors. E-mail: roberto.gobetto@unito.it., dbraga@ciam.unibo.it, r.k.harris@durham.ac.uk.
† Università di Torino.
‡ Università di Bologna.
§ Università di Sassari.
|| University of Durham.

(1) Hibbert, F.; Emsley, J. *Adv. Phys. Org. Chem.* **1990**, *26*, 255−391.
(2) Jeffrey, A. G. *An Introduction to Hydrogen Bonding*; Oxford University Press: New York, 1997.
(3) Kawahara, S.; Uchimaru, T. *Eur. J. Org. Chem.* **2003**, 2577−2584.
(4) Alkorta, I.; Elguero, J. *J. Phys. Chem. B* **2003**, *107*, 5306−5310.
(5) Cheng, A. C.; Chen, W. W.; Fuhrmann, C. N.; Frankel, A. D. *J. Mol. Biol.* **2003**, *327*, 781−796.
(6) Tarui, M.; Nomoto, N.; Hasegawa, Y.; Minoura, K.; Doi, M.; Ishida, T. *Chem. Pharm. Bull.* **1996**, *44*, 1998−2002.
(7) Ueda, H.; Iyo, H.; Doi, M.; Inoue, M.; Ishida, T. *Biochim. Biophys. Acta* **1991**, *1075*, 181−186.
(8) Lodi, P. J.; Knowles, J. R. *Biochemistry* **1991**, *30*, 6948−6956.
(9) Mezei, G.; Raptis, R. G. *New J. Chem.* **2003**, *27*, 1399−1407.
(10) Li, X. Z.; Liao, D. Z.; Jiang, Z. H.; Yan, S. P. *Transition Met. Chem.* **2003**, *28*, 506−510.
(11) Li, J. R.; Du, M.; Bu, X. H.; Zhang, R. H. *J. Solid State Chem.* **2003**, *173*, 20−26.
(12) Beginn, U. *Prog. Polym. Sci.* **2003**, *28*, 1049−1105.
(13) Desiraju, G. R. *J. Mol. Struct.* **2003**, *656*, 5−15.
(14) Etter, M. C. *Acc. Chem. Res.* **1990**, *23*, 120−126.
(15) Zaworotko, M. J. *Nature* **1997**, *386*, 220−221.
(16) Jeffrey, A. G.; Saenger, W. *Hydrogen Bonding in Biological Structures*; Springer-Verlag: Berlin, 1991.
(17) Prins, L. J.; Reinhoudt, D. N.; Timmerman, P. *Angew. Chem. Int. Ed.* **2001**, *40*, 2383−2426.
(18) Gilli, G.; Gilli, P. *J. Mol. Struct.* **2000**, *552*, 1−15.
(19) Steiner, T. *Angew. Chem. Int. Ed.* **2002**, *41*, 48−76.
(20) Desiraju, G. R. *Acc. Chem. Res.* **2002**, *35*, 565−573.
(21) Braga, D.; Maini, L.; Polito, M.; Grepioni, F. *Struct. Bonding* **2004**, *111*, 1−32.
(22) Bernstein, J.; Davis, R. E.; Shimoni, L.; Chang, N. L. *Angew. Chem., Int. Ed. Engl.* **1995**, *34*, 1555−1573.

10.1021/cm049063x CCC: $30.25
Published on Web 02/26/2005

and whether they are in the gas phase or in solution.[23−30] The enthalpies of weak hydrogen bonds involving oxygen and nitrogen are in the range 16−40 kJ mol^{-1},[31] but it has been reported for LBHBs that the strength is about 50−100 kJ mol^{-1}.[32]

Several techniques have been used for the detection and characterization of the hydrogen bond. Neutron diffraction crystallography is certainly the most definitive way to detect such interactions, but low-temperature X-ray crystallography can also be used.[33,34] In weak hydrogen bonds the heavy atoms are separated by less than the sum of their van der Waals radii i.e., for O···H···O ≤ 2.6 Å, for N···H···N ≤ 2.8 Å, and for N···H···O ≤ 2.7 Å, whereas in strong HB the heavy-atom separations are 2.4−2.55 Å for O···H···O, 2.6−2.7 Å for N···H···N, and 2.5−2.6 Å for N···H···O.[32] The various techniques have some intrinsic limitations and cannot be universally applied. This is, for example, the case of a polycrystalline powder obtained from solvent-free reactions such as those occurring in the solid state between molecules, or between two solids, or between a solid and a gas. For these kinds of reactions, which are important from both the environmental and topochemical viewpoints, the alternative investigation techniques are mainly IR and NMR spectroscopy. The typical evidence of the weak hydrogen bond is the high-frequency shift of the ^{1}H NMR data and the red shift in vibrational spectroscopy.[35,36] For strong HB the infrared bands are very broad and shifted to longer wavelengths and their ^{1}H signals are far higher in frequency than those normally associated with weak hydrogen bonds, 16−22 ppm for strong hydrogen bonds to nitrogen or oxygen and 16 ppm for [F···H···F]$^-$.[1]

In the solid state, HBs have been investigated by different spectroscopic approaches. The development of line narrowing techniques in solids, i.e., the possibility of spinning the sample (MAS) at rates higher than 20 kHz allows the location of chemical shifts of protons in HB leading to an increasing number of ^{1}H studies.[37−39] It has been shown[40−42] that the plot of the chemical shifts vs bond lengths is useful for obtaining the positions of the hydrogen atoms. Furthermore, hydrogen bond interactions have been studied by cross polarization magic angle spinning (CPMAS) ^{13}C and ^{15}N spectroscopy.[43−48] Isotropic ^{13}C chemical shifts linearly increase with decreasing N−O distances whereas ^{13}C chemical shift tensors of carbonyl carbon atoms of l-alanine residues in peptides, determined by spinning sideband pattern analysis, are a clear indication of the presence of a hydrogen bond interaction.[44]

It is known that the ^{15}N chemical shift range is wider and more sensitive to the presence of the hydrogen bond than that of ^{13}C.[49] ^{15}N NMR studies have shown that molecular association in the liquid state or in the solid state through intermolecular hydrogen bonds produces a high-frequency or low-frequency shift according to the type of nitrogen atom and the type of interaction.[50−53] For example, aliphatic amines involved in hydrogen bonds show in solution a high-frequency shift of 1−5 ppm when interacting with donor solvents, whereas the high-frequency shift is of the order of 10−25 ppm in the case of protonating solvents.[52,53]

Because in the solid state the signals are not averaged by solvent effects or by rapid exchange processes often present in solution, the change in the nitrogen chemical shifts caused by complete protonation can be of the order of 50−100 ppm, allowing a more accurate study.[54]

For glycine residues in solid oligopeptides, a relationship between the N−O distance and the ^{15}N chemical shift tensor in C═O···H−N hydrogen bonds has been found.[55] In this case, it is δ_{33} that shows a linear correlation with the N−O distance, whereas δ_{11} and δ_{22} are nearly independent.

We previously reported the results of a systematic investigation of the reaction in solution and in the solid state between a tertiary amine base, namely 1,4-diazabicyclo[2.2.2]-octane (dabco), **1**, with a series of dicarboxylic organic acid

(23) Xia, A. B.; Knox, J. E.; Heeg, M. J.; Schlegel, H. B.; Winter, C. H. *Organometallics* **2003**, *22*, 4060−4069.
(24) LeGreve, T. A.; Loh, A. P. *Biophys. J.* **2003**, *84*, 498A.
(25) Khaikin, L. S.; Grikina, O. E.; Golubinskii, A. V.; Vilkov, L. V.; Atavin, E. G.; Asfin, R. E.; Denisov, G. S. *Dokl. Phys. Chem.* **2003**, *390*, 158−162.
(26) Buemi, G. *Chem. Phys.* **2002**, *282*, 181−195.
(27) Kumar, G. A.; McAllister, M. A. *J. Org. Chem.* **1998**, *63*, 6968−6972.
(28) Chen, J. G.; McAllister, M. A.; Lee, J. K.; Houk, K. N. *J. Org. Chem.* **1998**, *63*, 4611−4619.
(29) Mehring, M.; Schurmann, M.; Ludwig, R. *Chem. Eur. J.* **2003**, *9*, 838−849.
(30) Chen, J. Y. J.; Naidoo, K. J. *J. Phys. Chem. B* **2003**, *107*, 9558−9566.
(31) Pauling, L. *The Nature of The Chemical Bond*; Cornell University Press: Ithaca, NY, 1960.
(32) Frey, P. A. *Magn. Reson. Chem.* **2001**, *39*, S190−S198.
(33) Ranganathan, A.; Kulkarni, G. U.; Rao, C. N. R. *J. Mol. Struct.* **2003**, *656*, 249−263.
(34) Hertweck, B.; Libowitzky, E.; Schultz, A. J. *Z. Kristallogr.* **2003**, *218*, 403−412.
(35) Garcia-Viloca, M.; Gelabert, R.; Gonzalez-Lafont, A.; Moreno, M.; Lluch, J. M. *J. Phys. Chem. A* **1997**, *101*, 8727−8733.
(36) Nakanaga, T.; Buchhold, K.; Ito, F. *Chem. Phys.* **2003**, *288*, 69−76.
(37) Brus, J.; Dybal, J. *Macromolecules* **2002**, *35*, 10038−10047.
(38) Brus, J.; Dybal, J.; Sysel, P.; Hobzova, R. *Macromolecules* **2002**, *35*, 1253−1261.
(39) Lorente, P.; Shenderovich, I. G.; Golubev, N. S.; Denisov, G. S.; Buntkowsky, G.; Limbach, H. H. *Magn. Reson. Chem.* **2001**, *39*, S18−S29.
(40) Berglund, B.; Vaughan, R. W. *J. Chem. Phys.* **1980**, *73*, 2037.
(41) Yamauchi, K.; Kuroki, S.; Ando, I. *J. Mol. Struct.* **2002**, *602*, 9−16.
(42) Harris, R. K.; Jackson, P.; Merwin, L. H.; Say, B. J.; Hägele, G. *J. Chem. Soc., Faraday Trans.* **1988**, *84*, 3649.
(43) Gu, Z. T.; McDermott, A. *J. Am. Chem. Soc.* **1993**, *115*, 4282−4285.
(44) Gu, Z. T.; Zambrano, R.; McDermott, A. *J. Am. Chem. Soc.* **1994**, *116*, 6368−6372.
(45) Facelli, J. C.; Gu, Z. T.; McDermott, A. *Mol. Phys.* **1995**, *86*, 865−872.
(46) Aguilar-Parrilla, F.; Scherer, G.; Limbach, H. H.; Focesfoces, M. D. C.; Cano, F. H.; Smith, J. A. S.; Toiron, C.; Elguero, J. *J. Am. Chem. Soc.* **1992**, *114*, 9657−9659.
(47) Aguilar-Parrilla, F.; Limbach, H. H.; Elguero, J.; Foces-Foces, C.; Scherer, G.; Cano, F. H.; Smith, J. A. S.; Toiron, C.; Wehrle, B.; Baldy, A.; Pierrot, M.; Khurshid, M. M. T.; Larcombe-McDouall, J. B. *J. Am. Chem. Soc.* **1989**, *111*, 7304.
(48) Aguilar-Parrilla, F.; Claramunt, R. M.; Lopez, C.; Sanz, D.; Limbach, H. H.; Elguero, J. *J. Phys. Chem.* **1994**, *98*, 8752−8760.
(49) Levy, G. C.; Lichter, R. L. *Nitrogen-15 Nuclear Magnetic Resonance Spectroscopy*; Wiley: New York, 1979.
(50) Litchmann, W. M.; Alei, M., Jr.; Florin, A. E. *J. Am. Chem. Soc.* **1969**, *91*, 6574.
(51) Litchmann, W. M.; Alei, M., Jr.; Florin, A. E. *J. Am. Chem. Soc.* **1970**, *92*, 4828.
(52) Duthaler, R. O.; Roberts, J. D. *J. Magn. Reson.* **1979**, *34*, 129.
(53) Botto, R. E.; Roberts, J. D. *J. Org. Chem.* **1977**, *42*, 2247.
(54) Foces-Foces, C.; Echevarria, A.; Jagerovic, N.; Alkorta, I.; Elguero, J.; Langer, U.; Klein, O.; Minguet-Bonvehi, M.; Limbach, H. H. *J. Am. Chem. Soc.* **2001**, *123*, 7898−7906.
(55) Fukutani, A.; Naito, A.; Tuzi, S.; Saito, H. *J. Mol. Struct.* **2002**, *602*, 491−503.

molecules of increasing aliphatic chain length, $HOOC(CH_2)_n$-COOH ($n = 1-7$).[56] We demonstrated that the measurement of the carbon chemical shift tensors of the COOH group obtained by sideband intensity analysis of ^{13}C CPMAS NMR spectra obtained at low spin rates represents a potential tool for the investigation of the position of the hydrogen in these supramolecular adducts.

The interest in extending such an approach to ^1H MAS and ^{15}N CPMAS NMR lies in the fact that these two nuclei are directly involved in the formation of hydrogen bonds, and therefore are more sensitive probes to the hydrogen position. An integrated theoretical and experimental approach can be successfully applied to overcome difficulties in the characterization.[57−59] For these reasons, our investigation is supported by theoretical DFT calculations of NMR parameters, to find (a) a correlation between both the ^1H and ^{15}N chemical shifts of the atoms involved in the hydrogen bond and the structural parameters previously obtained by X-ray analysis, and (b) a correlation between the H/D isotopic effects on the ^{15}N chemical shift and the geometries and strengths of hydrogen bonds.

2. Experimental Section

2.1 Chemicals and Reagents. Dabco and dicarboxylic acids $HOOC(CH_2)_nCOOH$ have been purchased from Aldrich and used without further purification. All the adducts were prepared by solid-state synthesis. In a typical reaction, equimolar quantities of dabco and the dicarboxylic acid were manually ground in an agate mortar. In all cases the characterization of the compounds has been confirmed by the full agreement of the X-ray powder diffractograms with the data previously reported.[56] The deuterated compounds were prepared by dissolving 200 mg of the corresponding protonated acid in D_2O (99.8% enriched, Aldrich) for 1 h to achieve complete deuteration, followed by evaporation of the solvent. The disappearance of the COOH signal in the ^1H NMR spectra confirmed the complete deuteration of the acids. The deutero-acid was dissolved in 99.9% EtOD (25 mL, Aldrich) and then an equimolar quantity of dabco was added. The suspension was stirred at 50 °C until complete dissolution. The solution was allowed to cool slowly to room-temperature overnight, yielding colorless crystals.

2.2 NMR Spectra. Proton measurements were mostly performed on a Varian InfinityPlus 500 spectrometer operating at 499.7 MHz for ^1H. Powdered samples were spun at 28 kHz in a Varian 2.5-mm HX probe. Spectra were acquired using a $\pi/2$ pulse of 3.8 μs in duration and a pulse delay of 20 s over a spectral width of 100 kHz. A total of 4 transients was collected for each spectrum. Proton chemical shifts were referenced via the resonance of PDMSO (polydimethylsiloxane) at 0.14 ppm relative to TMS. The second-order splitting for signals from H−N protons were obtained using a Varian Unity Inova 300 spectrometer operating at 299.82 MHz.

^{15}N spectra were recorded on a JEOL GSE 270 spectrometer equipped with a Doty probe operating at 27.25 MHz for ^{15}N. Powdered samples were spun at 4−5 kHz. A contact time of 5 ms, a repetition time of 15 s, and a spectral width of 35 kHz were used for accumulation of 3000−4000 transients. ^{15}N chemical shifts were referenced via the resonance of solid $(NH_4)_2SO_4$ (−355.8 ppm with respect to CH_3NO_2[60]).

Some of the spectra were performed at low and high temperatures, but no spectral changes could be observed. Low-temperature measurements were carried out by passing nitrogen gas through a heat exchanger immersed in liquid nitrogen, thus allowing temperature as low as 213 K to be achieved, maintaining the spin rate between 2.5 and 3 kHz (enough for obtaining spectra essentially free from spinning sidebands).

2.3 Calculations. We used density functional theory (DFT) calculations throughout, adopting Becke's three-parameter hybrid function[61] and Lee−Yang−Parr's gradient-corrected correlation function[62] ("B3LYP") method. Geometry optimizations have been performed in two steps by means of the Jaguar program,[63] first using a 6-31G** basis set, and in the second step using a 6-311++G** basis set. The geometry scans, i.e., calculation on geometries in which only the HB hydrogen atom is moved along the N−O axis, have been carried out by Jaguar at the 6-311++G** level on the optimized structures. The NMR shielding parameters were calculated starting from the optimized geometries, by means of the gauge-including atomic orbital (GIAO) method as implemented in the Gaussian 98 program,[64] and employing the 6-311++G-(2d,p) basis set. The absolute isotropic constant shielding for ^{15}N of dabco (226.4901), used as reference, has been calculated from the reported neutron diffraction structure of the ligand.[65] To take in account the nearest-neighbor effects in the solid-state, the calculated ^{15}N absolute shielding has been extracted from the central of three aligned dabco molecules. Thenceforward, the ^{15}N chemical shift values were referenced according to the known experimental value of the dabco base (−14.4 ppm) following the equation $\delta_s = 226.4901 - \sigma_s - 14.4$ (where the subscript "s" refers to the sample). The ^1H and ^{13}C chemical shifts were calculated in the same way but have been referred to the computed shielding for TMS optimized at B3LYP/6-311++G(2d,p) (absolute isotropic constant shielding values of 31.8194 and 182.4560 for ^1H and ^{13}C, respectively). The ^{15}N and ^{13}C principal tensor components are reported following the Haeberlen convention[66] where $|\delta_{33} - \delta_{iso}| \geq |\delta_{11} - \delta_{iso}| \geq |\delta_{22} - \delta_{iso}|$ and the shielding anisotropy is defined as $\Delta\sigma = \sigma_{33} - (\sigma_{11} + \sigma_{22})/2$ with $|\sigma_{33} - \sigma_{iso}| \geq |\sigma_{11} - \sigma_{iso}| \geq |\sigma_{22} - \delta_{iso}|$.

3. Results and Discussion

The solid-state structures of seven adducts corresponding to the general formula $[N(CH_2CH_2)_3N]-H-[OOC(CH_2)_n$-

(56) Braga, D.; Maini, L.; de Sanctis, G.; Rubini, K.; Grepioni, F.; Chierotti, M. R.; Gobetto, R. *Chem. Eur. J.* **2003**, *22*, 5538−5548.
(57) Harris, R. K.; Ghi, P. Y.; Hammond, R. B.; Ma, C. Y.; Roberts, K. J. *J. Chem. Soc., Chem. Commun.* **2003**, 2834−2835.
(58) Nervi, C.; Gobetto, R.; Milone, L.; Viale, A.; Rosenberg, E.; Rokhsana, D.; Fiedler, J. *Chem. Eur. J.* **2003**, *9*, 5749−5756.
(59) Gobetto, R.; Nervi, C.; Romanin, B.; Salassa, L.; Milanesio, M.; Croce, G. *Organometallics* **2003**, *22*, 4012−4019.
(60) Schilf, W.; Kamienski, B.; Dziembowska, T. *J. Mol. Struct.* **2002**, *602*, 41−47.
(61) Becke, A. D. *J. Chem. Phys.* **1993**, *98*, 5648−5652.
(62) Lee, C.; Yang, W.; Parr, R. G. *Phys. Rev. B: Condens. Matter* **1988**, *37*, 785.
(63) Jaguar 5.0. Schrodinger, LLC: Portland, Oregon, 2002.
(64) Frisch, M. J.; Trucks, G. W.; Schlegel, H. B.; Scuseria, G. E.; Robb, M. A.; Cheeseman, J. R.; Zakrzewski, V. G.; Montgomery, J. A., Jr.; Stratmann, R. E.; Burant, J. C.; Dapprich, S.; Millam, J. M.; Daniels, A. D.; Kudin, K. N.; Strain, M. C.; Farkas, O.; Tomasi, J.; Barone, V.; Cossi, M; Cammi, R.; Mennucci, B.; Pomelli, C.; Adamo, C.; Clifford, S.; Ochterski, J.; Petersson, G. A.; Ayala, P. Y.; Cui, Q.; Morokuma, K.; Malick, D. K.; Rabuck, A. D.; Raghavachari, K.; Forestman, J. B.; Cioslowski, J.; Ortiz, J. V.; Baboul, A. G.; Stefanov, B. B.; Liu, G.; Liashenko, A.; Piskorz, P.; Komaromi, I.; Gomperts, R.; Martin, R. L.; Fox, D. J.; Keith, T.; Al-Laham, M. A.; Peng, C. Y.; Nanayakkara, A.; Challacombe, M.; Gill, P. M. W.; Johnson, B.; Chen, W.; Wong, M. W.; Andres, J. L.; Gonzales, C.; Head-Gordon, M.; Replogle, E. S.; Pople, J. A. *Gaussian 98*, revision A.9; Gaussian, Inc.: Pittsburgh, PA, 1998.
(65) Nimmo, J. K.; Lucas, B. W. *Acta Crystallogr., Sect. B: Struct. Sci.* **1976**, *32*, 348−353.
(66) Haeberlen, U. High-Resolution NMR in Solids; In *Advances in Magnetic Resonance*; Waugh, J. S., Ed.; Academic Press: New York, 1976; Vol. 1.

Scheme 1. Crystal Structures of Compounds 1C3−1C9. Hydrogen Atoms Not Involved in HBs Are Omitted for Simplicity. White, Grey, and Shadowed Circles Represent Carbon, Oxygen, and Nitrogen Atoms, respectively. Small Circles Indicate the Hydrogen Atoms Involved in HBs

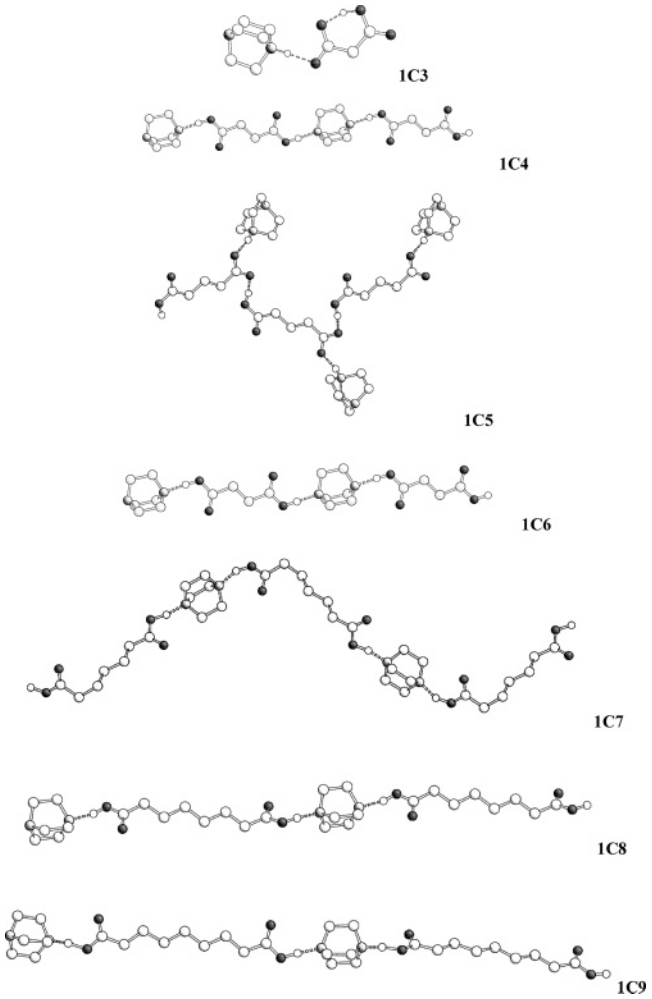

COOH] ($n = 1-7$) have been previously investigated by means of ^{13}C solid-state NMR and powder and single-crystal X-ray diffraction. In the following, we refer to the diacids by the total number of carbon atoms in the molecule, hence the adducts are identified as **1C3** for the dabco−malonic acid adduct, **1C4** for the dabco−succinic acid adduct, etc.

Two major supramolecular motifs have been observed in the crystal structures, namely the A/B/A/B chain (**1C4**, **1C6**, **1C7**, **1C8**, and **1C9**) whereby the base is inserted in the carboxylic chain of the parent diacid and the A/A/A/A chain with lateral bonds to the base B (**1C5**), except in the case of **1C3** where a 1:1 adduct is present (see Scheme 1). In all cases N···H···O hydrogen bond interactions are responsible for the formation of the acid−base adducts. The proton transfer process along a hydrogen bond may imply the transformation of a molecular crystal into a molecular salt.

On the basis of the diffraction and solid-state ^{13}C NMR data, compounds **1C3** and **1C5** have been described as salts (i.e., proton transfer from the acid to the base has occurred), whereas **1C4**, **1C6**, **1C7**, **1C8**, and **1C9** are better described as cocrystals (i.e., no proton transfer has occurred). The proton transfer appears to be the driving force for the different supramolecular structures. Then the different packing in **1C3** and **1C5** may be due to the protonation of the first nitrogen favored by the presence of the neighbor O−H···O HB interaction, which in turn changes the donor properties of the second nitrogen of dabco.[67]

3.1 NMR Characterization. The ^1H and ^{15}N chemical shifts of all compounds are reported in Table 1. The **1C3** ^1H spectrum run at 500 MHz shows two peaks in the HB region (Figure 1a): one at 12.4 ppm assigned to the $N^+-H\cdots O^-$ hydrogen (with proton transfer) while the other at 17.6 ppm is due to the hydrogen involved in the intramolecular O···H···O interaction. In the ^1H spectrum at 300 MHz (Figure 1b) the low-frequency peak splits into two signals (in the relative ratio 2:1). The observed splitting of 1.2 ppm (350 Hz) is due to a second-order effect of dipolar coupling to the quadrupolar nitrogen-14 nuclei, confirming the proposed assignment for the signal.[68] The ^1H chemical shift for the $N^+-H\cdots O^-$ interaction (12.4 ppm) and the N−O distance (2.703 Å), obtained by X-ray measurements, show that this is a weak HB; conversely the ^1H chemical shift and the O−O distance (2.455 Å) of the O···H···O bond fall in the range of the strong hydrogen bond.[1,32,42] The **1C5** spectrum is quite similar, showing two peaks at 12.2 and 16.4 ppm attributed to the protons involved in the $N^+-H\cdots O^-$ HB and in the intermolecular O···H···O interaction, respectively. The signal at δ 16.4 ppm is very broad ($\nu_{1/2} = 1032$ Hz) but changing the temperature (373 K) and the spinning speed (20 000 Hz) gave no significant differences in the line width. This is probably due to the lack of fully averaging the strong dipolar interaction between the CH_2 hydrogens of the acid and the O···H···O hydrogen ($r_{H-H} \approx 2.33$ Å). At 300 MHz the low-frequency peak behaves analogously to **1C3**, i.e., a split of 440 Hz into a doublet (in the relative ratio 2:1) centered at 12.5 ppm is observed. Although the **1C5** supramolecular motif is different from that of **1C3**, we can apply the same considerations: thus, the $N^+-H\cdots O^-$ interaction is classified as a weak HB while the intermolecular O···H···O is classified as a strong HB. The ^1H chemical shifts for the other compounds (**1C4**, **1C6**, **1C7**, **1C8**, and **1C9**) fall approximately in the same HB region (about 16−17 ppm) and all correspond to an N···H−O interaction (without proton transfer). In almost all cases, except **1C4** (Figure 2) and **1C8**, two signals are present in the ^1H spectrum corresponding to the crystallographic independent sites. This observation prompted us to tackle the problem of the correlation between ^1H chemical shifts and the different N−O distances. The correlation we propose is reported in Table 1. The compounds **1C4** and **1C8** show in the ^1H spectrum (as well as in the ^{15}N spectrum for **1C8**, see below) only one peak, although one should expect two signals corresponding to the two different N···H−O environments present in the two adducts. We suggest that the presence of a single peak is due to a casual overlapping. If one considers these ^1H chemical shifts and the N−O distances, which fall around 2.57 Å, these HBs can be

(67) Someswara Rao, N.; Babu Rao, G.; Murthy, B. N.; Maria Das, M.; Prabhakar, T.; Lalitha, M. *Spectrochim. Acta, Part A* **2002**, *58*, 2737−2757.
(68) Harris, R. K.; Olivieri, A. C. *Prog. Nucl. Magn. Reson. Spectrosc.* **1992**, *24*, 435−456.

Table 1. X-ray and NMR Data (Experimental and Calculated) for Compounds 1C3−1C9[a]

	Experimental					Calculated								
compound	N−O distance (Å)	δ ^{1}H (HB)	δ ^{15}N(H)	δ ^{15}N(D)	$^1\Delta^{15}$N(D) (ppm)	^{15}N $\Delta\sigma$ (ppm)	δ ^{15}N[b]	δ_{11}	δ_{22}	δ_{33}	N−H distance (Å)	O−H distance (Å)	N−H−O angle	note
dabco 1			−14.4	−14.4		−48.88	−14.4	−30.91	−30.54	18.15				free N
1C3	2.455(3)[c]	17.6[d]	−14.1	−14.1		−50.76	−15.6	−34.84	−30.12	18.28				free N
	2.703(3)	12.4	4.7	4.7		−12.33	10.2	5.69	6.43	18.39	1.100	1.604	177.4	N^+—H···O^-
1C4	2.588(4)	16.5	−7.2	−8.5	1.3	−32.94	−5.2	−17.81	−14.61	16.73	1.566	1.026	173.7	N···H—O
	2.557(5)	16.5	−4.4	−5.0	0.6	−32.10	−3.3	−16.28	−11.83	18.05	1.527	1.039	170.6	N···H—O
	2.556(5)													
	2.559(5)													
1C5	2.523(3)[c]	16.4[d]	−16.6	−16.6		−48.82	−17.9	−35.21	−33.30	14.56				free N
	2.697(3)	12.2	3.5	3.5		−10.46	8.0	3.41	5.69	15.01	1.104	1.607	168.2	N^+—H···O^-
1C6	2.594(5)	16.4	−6.5	−7.8	1.3	−32.75	−5.1	−18.81	−13.29	16.70	1.574	1.026	172.4	N···H—O
	2.558(5)	17.2	−2.5	−2.8	0.3	−29.96	−5.1	−15.30	−14.92	14.85	1.526	1.041	169.9	N···H—O
1C7	2.588(4)	15.6	−8.2	−9.3	1.1	−32.32	−5.8	−19.23	−13.96	15.72	1.569	1.024	172.8	N···H—O
	2.563(4)	16.4	−5.0	−5.7	0.7	−31.27	−2.9	−15.82	−10.89	17.91	1.532	1.031	179.4	N···H—O
1C8	2.595(4)	15.8	−6.6	−7.5	0.9	−31.80	−7.3	−21.49	−14.32	13.89	1.587	1.024	167.2	N···H—O
	2.571(4)	15.8				−30.95	−6.1	−17.18	−15.73	14.49	1.551	1.029	170.3	
1C9	2.548(3)	16.6	−4.7	−5.9	1.2	−31.26	−4.1	−15.97	−13.08	16.73	1.527	1.030	169.7	N···H—O
	2.605(3)	15.3	−8.4	−9.7	1.3	−32.10	−5.2	−17.24	−14.51	16.22	1.605	1.019	165.8	N···H—O

[a] The components of the chemical shift tensors are defined following the Haeberlen convention where $|\delta_{33} - \delta_{iso}| \geq |\delta_{11} - \delta_{iso}| \geq |\delta_{22} - \delta_{iso}|$ and $\Delta\sigma = \sigma_{33} - (\sigma_{11} + \sigma_{22})/2$ with $|\sigma_{33} - \sigma_{iso}| \geq |\sigma_{11} - \sigma_{iso}| \geq |\sigma_{22} - \delta_{iso}|$. [b] The scale of ^{15}N has been calculated relative to the absolute shielding of dabco, set to −14.4 ppm, according to the experimental value (see Experimental Section for details). [c] O−O distance (Å). [d] ^{1}H chemical shift for the O−H···O intramolecular HB (**1C3**) and for the O−H···O intermolecular HB (**1C5**).

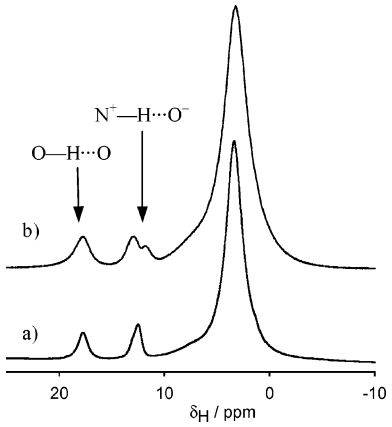

Figure 1. ^{1}H MAS NMR spectrum of **1C3** at 298 K obtained at 499.70 MHz (a) and at 300 MHz (b).

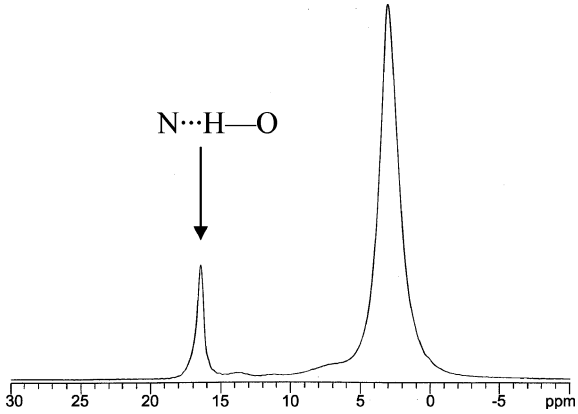

Figure 2. ^{1}H MAS NMR spectrum of **1C4** at 298 K obtained at 499.70 MHz.

defined as strong hydrogen bonds (as confirmed by the H/D isotope effect on the ^{15}N chemical shift, vide infra).

The ^{15}N CPMAS spectra of the free dabco and the adducts of formula $[N(CH_2CH_2)_3N]-H-[OOC(CH_2)_nCOOH]$ (n = 1−7) were measured at room temperature and the results are reported in Table 1. No differences in the chemical shifts

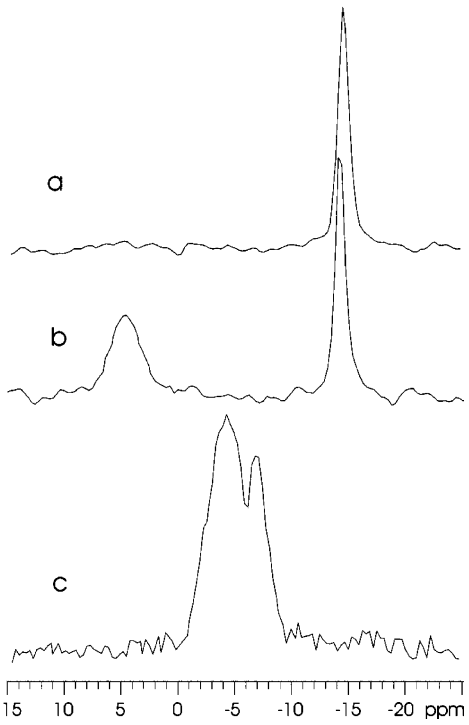

Figure 3. ^{15}N CPMAS NMR spectra of dabco (a), **1C3** (b), and **1C4** (c) at 298 K obtained at 27.25 MHz.

and line widths of the ^{15}N resonances have been observed by decreasing the temperature to 213 K.

For dabco only one sharp peak is observed at −14.4 ppm, indicating that the two nitrogen sites are equivalent (Figure 3a).

For solutions, the ^{15}N peak of dabco falls at 10.0 ppm in CCl_4, 11.6 ppm in EtOH, and 18.6 ppm in 1 M HCl (δ_{NH3} 0 ppm). Rao et al.[67] showed that the dabco in solution gives a single resonance for the two nitrogen atoms both in donor and acceptor solvents. They pointed out that the presence of a single signal is justified by the fast exchange occurring in solution (Scheme 2).

Scheme 2

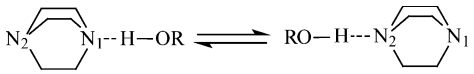

The comparisons among the values observed in different solvents show that in ethanol (a donor solvent) there is only a limited chemical shift change (1.6 ppm), whereas in the case of a protonating solvent, as for hydrochloric acid, the shift is much higher (8.6 ppm). These results are a clear indication that also in solution it is possible to discriminate, in the case of dabco, between protonated and nonprotonated nitrogen atoms.

From the data reported in Table 1 it is evident that the ^{15}N chemical shift of dabco in the different adducts spans a range more than 35 ppm. However, by comparing these data and the X-ray information we observed a good agreement between the number of peaks in the NMR spectrum and the number of the nitrogen atoms in crystallographically independent sites. Here we propose an assignment of each resonance to the different nitrogen environments. **1C3** reveals the presence of a sharp peak at −14.1 ppm and a relatively broader peak at 4.7 ppm (Figure 3b). Knowing that the nitrogen resonance for free dabco occurs at −14.4 ppm, we can assume that the signal at −14.1 ppm arises from the nitrogen atom not involved in the HB interaction, whereas the other peak is shifted to high frequency due to the presence of the $N^+-H\cdots O^-$ environment proposed on the basis of the X-ray data. Also, **1C5** shows a similar spectrum with the sharp peak at −16.6 ppm (dabco free nitrogen) and a slightly broader resonance at 3.5 ppm for the nitrogen atom involved in the intermolecular $N^+-H\cdots O^-$ interaction.

The ^{15}N spectra of **1C4** (Figure 3c), **1C6**, **1C7**, **1C8**, and **1C9** adducts are characterized by the presence of two signals (one in the case of **1C8** as previously observed in the ^{1}H spectrum) falling in the range between −4 and −8 ppm (see Table 1). Then almost in every case it was possible to discriminate among nonequivalent crystallographic sites characterized by different N−O distances and we propose on this basis a possible assignment. The ^{15}N spectrum of **1C4** shows two signals at −4.4 ppm and at −7.2 ppm in a ratio 3:1. The former is related to the three crystallographic independent sites having similar N−O distances of 2.558(5), 2.556(5), and 2.559(5) Å, while the latter is associated with the N−O distance of 2.588(4) Å. The **1C6** X-ray structure reveals the presence of a carboxylate group, characterized by a short N−O distance of 2.557(5) Å and a carboxylic group associated with a longer N−O interaction [2.594(5) Å].[21] On the basis of these data, **1C6** can be described as a salt. The ^{15}N NMR spectrum shows two resonances at −6.5 ppm and −2.5 ppm. The former value, associated with the longer N−O distance, is typical of a N···H−O interaction, in agreement with the X-ray data and with the values found for the other compounds. The latter value, associated with the shorter N−O bonding distance, is only a little shifted to high frequency, probably indicating a weaker N···H−O interaction due to the formation of a partially protonated carboxylate group. For the **1C7** adduct the two resonances at −8.2 ppm and at −5.0 ppm are associated with the N−O distances of 2.588(4) Å and 2.563(4) Å, respectively, while **1C8** shows only one signal at −6.6 ppm, probably because of the nearly identical chemical environment of the two nitrogen atoms. The ^{15}N CPMAS spectrum of the **1C9** adduct has two resonances at −4.4 and −8.8 ppm, corresponding to the N−O values of 2.548(3) Å and 2.605(3) Å, respectively.

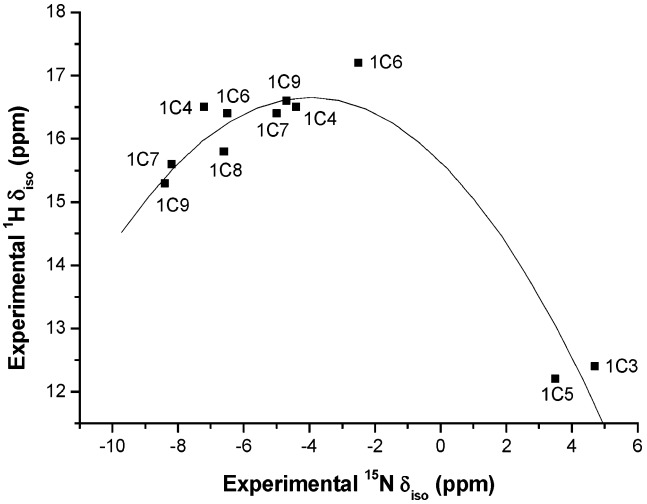

Figure 4. Plot of the experimental ^{1}H chemical shift vs the experimental ^{15}N chemical shift of the nitrogen atoms involved in HB for supramolecular adducts **1C3**−**1C9**.

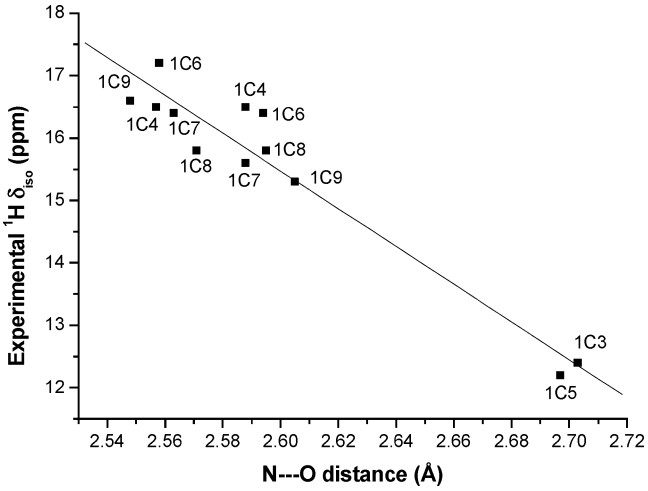

Figure 5. Plot of the experimental ^{1}H chemical shift vs the N−O distance for supramolecular adducts **1C3**−**1C9**.

On the basis of these results we are able to discriminate in the **1C3**−**1C9** series between free nitrogen atom, hydrogen-bonded nitrogen (N···H−O), and proton transfer ($N^+-H\cdots O^-$) cases. We can conclude the following: (*a*) the signals falling around −15 ppm are assigned to nitrogen atoms of dabco not involved in the hydrogen bond; (*b*) the resonances in the range −2 to −8 ppm are related to N···H−O contacts; and (*c*) a high-frequency shift of about 20 ppm indicates the presence of $N^+-H\cdots O^-$ interactions. Here are also reported the plots of δ_H *vs.* δ_N (Figure 4) and δ_H vs N−O distance (Figure 5). The former suggests a polynomial fit as previously observed by other authors[69,70] while the latter displays an approximately linear fit. Since

(69) Smirnov, S. N.; Benedict, H.; Golubev, N. S.; Denisov, G. S.; Kreevoy, M. M.; Schowen, R. L.; Limbach, H. H. *Can. J. Chem.* **1999**, *77*, 943−949.

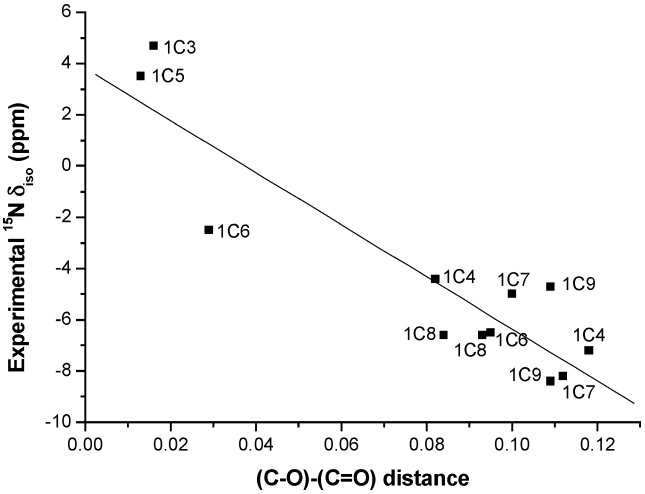

Figure 6. Plot of the experimental ^{15}N chemical shift of the nitrogen atoms involved in HB vs the difference between C−O and C═O distances of the carboxylic group for compounds **1C3**−**1C9**.

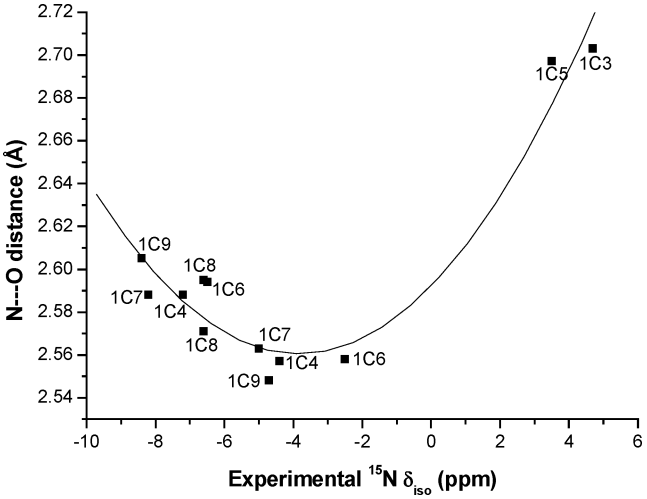

Figure 7. Plot of the experimental ^{15}N chemical shift of the nitrogen atoms involved in HB vs the N−O distance for compounds **1C3**−**1C9**.

Table 2. pK_a Values of the Dicarboxylic Acids

compound	pK_{a1}	pK_{a2}
malonic	2.83	5.69
succinic	4.16	5.61
glutaric	4.34	5.27
adipic	4.43	5.28
pimelic	4.51	5.31
suberic	4.52	5.73
azelic	4.55	5.41

the pK_a values of the dicarboxylic acids span only a limited range (Table 2), the plots cannot display a complete fitting as observed for example by Limbach, whose compounds had a pK_a range from 1 to 23.[69] However, it is possible to detect in both plots two well-defined regions, one related to strong (N···H−O) and the other related to weak (N^+−H···O^-) hydrogen bonds.

The ability of the ^{15}N CPMAS NMR to discriminate between proton transfer and hydrogen bridging is also more evident if one relates the ^{15}N parameters and the structural data: there is, in fact, a clean separation among the adducts defined as salts (**1C3** and **1C5**) and the structures defined as cocrystals (**1C4**, **1C7**, **1C8**, and **1C9**) if one considers either the relation between ^{15}N chemical shifts and the differences between C−O and C═O distances of the carboxylic group (Figure 6) or the relation between ^{15}N chemical shifts and the N−O distances (Figure 7). The relation between ^{15}N chemical shift and the N−O distance shows that N^+−H···O^- and N···H−O interactions correspond to long N···O distances while N···H···O interactions relate to shorter N···O distances as confirmed by the literature.[69,71]

3.2 DFT Calculations. With the aim to obtain more detailed and sound information, we performed three different DFT calculations on the complexes under study: (*i*) geometry optimizations by means of Jaguar, (*ii*) calculations of the NMR absolute chemical shifts using Gaussian 98, and (*iii*) geometry scans using Jaguar, which consists of sketching the energy as a function of the H position along the N−O axis defining the HB interaction (see experimental part). Geometry optimizations are usually carried out on a single molecule in the gas phase, more rarely simulating the presence of a solvent. In our case, however, we have to take into account that the acid/base pairs in the crystal packing strongly feel the presence of neighboring molecules, which are responsible for a well-defined force field. Therefore, geometry optimization performed either in the gas phase or in solution does not provide a suitable model for our purposes. Although periodic calculations could be performed using specialized software,[72,73] we preferred a simpler computational approach, i.e., to start from the corresponding X-ray refined structures, and to optimize the positions of the hydrogen atoms only. This appears to be a reasonable approximation, since the positions of heavy atoms are well established by X-ray structural analysis. A similar approach has been already successfully pursued.[57] Focusing our interest on the computation of magnetic properties of ^{1}H, ^{13}C, and ^{15}N nuclei, a dabco unit as well as all its corresponding adjacent acid molecules in the vicinal crystallographic cells have been selected for DFT calculations. This means a single molecule of acid in the case of **1C3**, two acid molecules facing the two nitrogens of dabco for **1C4**, **1C6**, **1C7**, **1C8**, and **1C9**, and two nearby acid molecules facing a single dabco nitrogen for **1C5**, according to the published X-ray structures.[56]

The optimized structures are then used to compute the chemical shifts by means of the GIAO method at B3LYP/6-311++G(2d,p) level (see Table 1). We also used the method of Harris et al.[57] to refine the hydrogen atom positions within HBs, in which the computed ^{1}H δ are reported as a function of the O−H distance while all other atoms are retained at their positions. Using the experimental δ value of 16.5 ppm, the plot for **1C4** (Figure 8) gives an O−H distance of 1.043 Å, which is in good agreement with the value obtained by geometry optimization (1.039 Å, Table 1). The same approach applied to **1C3** provides an O−H distance of 1.672 Å, which should be compared with 1.604 Å of Table 1. This slight difference can be explained, for this particular case, in terms of the adjacent intramolecular

(70) Benedict, H.; Limbach, H. H.; Wehlan, M.; Fehlhammer, W. P.; Golubev, N. S.; Janoschek, R. *J. Am. Chem. Soc.* **1998**, *120*, 2939−2950.
(71) Steiner, T. *J. Chem. Soc., Chem. Commun.* **1995**, 1331−1332.
(72) Goward, G. R.; Sebastiani, D.; Schnell, I.; Spiess, H. W.; Kim, H. D.; Ishida, H. *J. Am. Chem. Soc.* **2003**, *125*, 5792−5800.
(73) Sebastiani, D. *Mod. Phys. Lett. B* **2003**, *17*, 1301−1319.

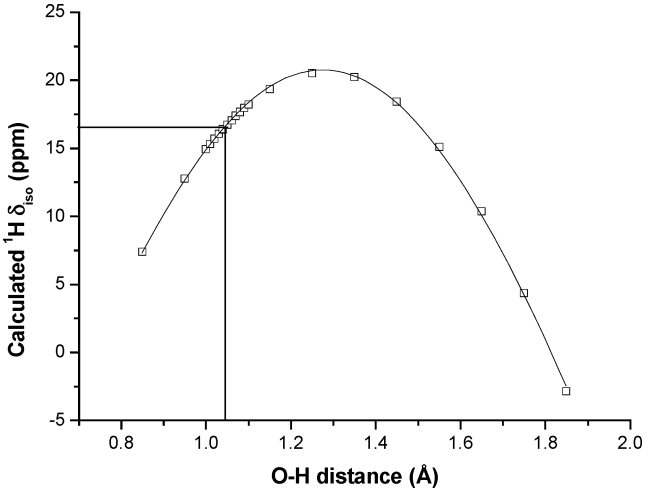

Figure 8. Plot of the calculated ^{1}H chemical shift for **1C4** vs O−H distance. The curve represents an empirical fit to a Gaussian equation.

O···H−O interaction, which plays a key role in defining the electron-withdrawing properties of the oxygen atom involved in the N^+−H···O^- interaction.

The B3LYP DFT method used for geometry optimization is well-known to systematically underestimate the HB energies (see for example ref 74 and references therein) and the problem is amplified in the computation of the shielding constants.[74−79] As a consequence, our calculated ^{1}H chemical shifts of HBs present an intrinsic error of the order of 0.4−2.7 ppm (see Supporting Information). Nevertheless the approach used in Figure 8 is still valid, since in this case the position of the H was arbitrarily set and therefore it is not affected by the use of the B3LYP DFT method.

For the ^{15}N analysis, although there is an underestimation of the calculated chemical shift in all cases with respect to the experimental data, the errors are reasonable if one considers the large δ range of the ^{15}N nuclei. It is worth noting that the trend of the influence of the HB interaction on the ^{15}N chemical shifts is maintained in the calculated data (−20 ppm for free nitrogen, −2.5 to −11 ppm for N···H−O interaction and +3 to +5 ppm for N^+−H···O^- interaction).

A better correlation can be obtained by considering the principal elements of the nuclear chemical shift tensor δ_{11}, δ_{22}, and δ_{33}. The interdependences among ^{15}N chemical shifts, ^{15}N anisotropies, and the type of HB are outlined in Figure 9.

As discussed in previous papers,[39,56] δ_{11}, δ_{22}, and δ_{33} of the nucleus directly involved with the localization of the intermolecular hydrogen bond are more sensitive to the change in the molecular structure,[77] and so may represent an interesting tool for the investigation of HB interactions. The calculated δ_{11}, δ_{22}, and δ_{33} values for ^{15}N exhibit an approximately linear relation with the corresponding experimental isotropic chemical shifts. As expected, the absolute value of the shielding anisotropy $|\Delta\sigma|$ significantly decreases on passing from a free nitrogen atom (48−50 ppm), to a N···H−O (30−33 ppm) and to a N^+−H···O^- interaction (≈11 ppm), showing a linear relationship with the experimental ^{15}N δ_{iso} values. In the case of **1C3** and **1C5**, the structures are better described by N^+−H···O^- interactions, in which the N−H distances are 1.100 and 1.104 Å respectively (O−H being 1.604 and 1.607 Å), whereas for **1C4**, **1C6**, **1C7**, **1C8**, and **1C9** the computed geometries are close to those expected for cocrystals rather than salts. Figures 7 and 9 suggest that **1C6** faces an intermediate situation between carboxylic and carboxylate state.

The comparison of ^{15}N chemical shift tensors obtained from the DFT method with the experimental data would require an expensive procedure of ^{15}N enrichment of the samples. However, the tensor component values for ^{13}C (previously reported in ref 56) match very well with the calculated parameters (see Supporting Information), supporting the theoretical ^{15}N tensor trends.

The relative energies of the optimized **1C3** and **1C4** molecules obtained by geometry scans, in which only the hydrogen is moved along the N−O axis, are reported in Figure 10 as a function of the O−H distance. To allow a direct comparison of the relative energies of **1C3** and **1C4** adducts, the lowest minima of the two curves have been arbitrarily set at zero energy.

The picture shows that two well-defined minima of energy exist for **1C3**, corresponding to the protonated (right) and the nonprotonated (left) forms. In this case the two local minima are found at ∼1.075 Å and 1.604 Å (O−H distances), the second corresponding to the N^+−H···O^- structure being more stable by about 10.0 kJ mol^{-1}, and with a calculated energy barrier of about 16.7 kJ mol^{-1} (trivially small with respect to RT) for the process N^+−H···O^- → N···H−O. A steeper minimum located at 1.031 Å is found in the case of **1C4**. For the **1C3** adduct the minimum of the energy is found when the hydrogen is closer to the N of dabco instead of the O of the acid, whereas the opposite holds for **1C4**. This is in agreement with the experimental data acquired from solid-state NMR investigations. It is worth noting that, for example, with an energy penalty of about 20.9 kJ mol^{-1}, the H in **1C3** is free to move from ca. 0.98 to 1.73 Å, whereas in the case of **1C4**, a narrower range is found (from 0.93 to 1.27 Å). The computed potential wells should be seen as an approximation, since we did not consider the extensive vibrational averaging that occurs for H-bonding. Furthermore, while the experimental chemical shift is the result of an average of the all-different H positions, the calculated chemical shifts are obtained from a single well-defined structure.

3.3 Hydrogen/Deuterium Isotope Effect. To improve the understanding of the hydrogen bond an investigation of the hydrogen/deuterium (H/D) isotope effect was performed by measuring the ^{15}N CPMAS spectra of the deuterated com-

(74) Ireta, J.; Neugebauer, J.; Scheffler, M. *J. Phys. Chem. A* **2004**, *108*, 5692−5698.
(75) Hinton, J. F.; Wilson, R. C. *Theoretical Treatments of Hydrogen Bonding*; J. Wiley & Sons Ltd.: New York, 1997.
(76) Stare, J.; Jezierska, A.; Ambrozic, G.; Kosir, I. J.; Kidric, J.; Koll, A.; Mavri, J.; Hadzi, D. *J. Am. Chem. Soc.* **2004**, *126*, 4437−4443.
(77) Helgaker, T.; Jaszunski, M.; Ruud, K. *Chem. Rev.* **1999**, *99*, 293−352.
(78) Smith, E. D. L.; Hammond, R. B.; Jones, M. J.; Roberts, K. J.; Mitchell, J. B. O.; Price, S. L.; Harris, R. K.; Apperley, D. C.; Cherryman, J. C.; Docherty, R. *J. Phys. Chem. B* **2001**, *105*, 5818−5826.
(79) Benedict, H.; Hoelger, C.; Aguilar-Parrilla, F.; Fehlhammer, W. P.; Wehlan, M.; Janoschek, R.; Limbach, H. H. *J. Mol. Struct.* **1996**, *378*, 11−16.

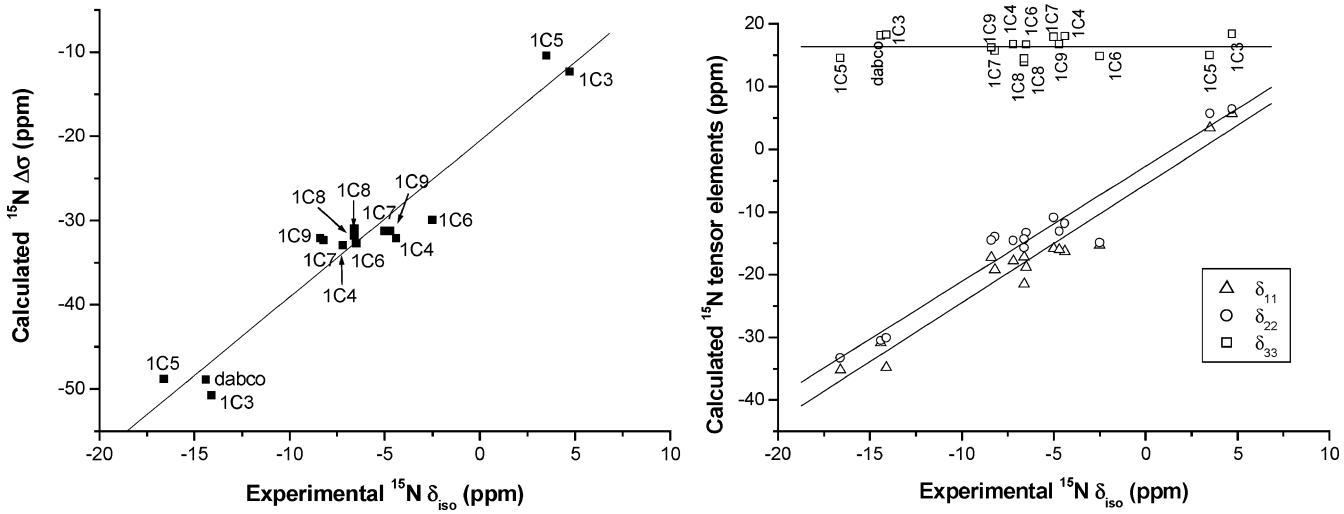

Figure 9. Calculated shielding anisotropy $\Delta\sigma$ (left) and calculated chemical shift tensors δ_{11}, δ_{22}, δ_{33} (right) as a function of the experimental isotropic ^{15}N chemical shift.

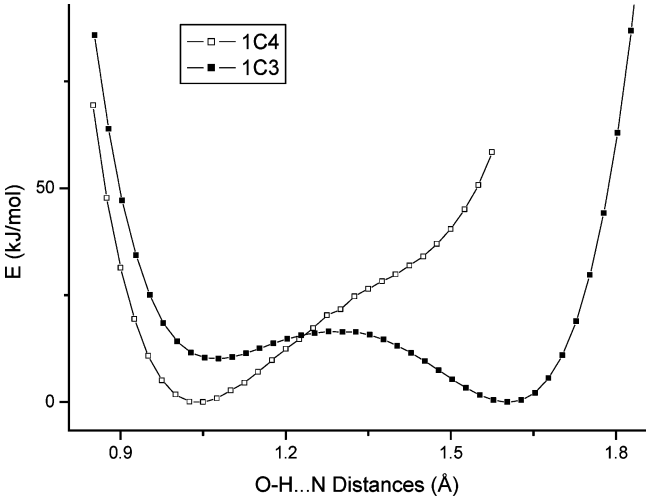

Figure 10. Relative energies at 6-311++G** level computed during geometry scans (O−H distances for the optimized geometries of **1C3** and **1C4**).

pounds (**1C3-d**, **1C4-d**, etc.) obtained from deuteron isotopic exchange of the carboxylic protons. Although only a few studies on the deuterium isotope effect in the solid state have been reported[39,70,79−81] this is potentially a useful parameter for the investigation of strong HB.

It has been shown by several authors,[82−84] that the replacement of the HB proton by a deuteron leads to a geometric isotope effect. We shall consider a generic A···H···B hydrogen bond (see Scheme 3, where q_1 is the distance of the proton with respect to the HB center and q_2 is the heavy atoms distance A···B).

It has been suggested that there is a primary and a secondary geometric influence on the H/D isotope effect. The former refers to the different positions of the proton and of the deuteron with respect to the center of the A- - -B

Scheme 3

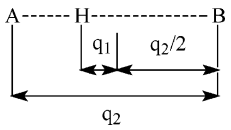

interaction, i.e., q_1 value, whereas the latter refers to the change of the distance (q_2) between heavy atoms, distance (q_2). When the hydrogen is replaced by a deuterium the smaller heavy atom−hydrogen distance decreases but the larger distance increases even more, leading to a widening of the hydrogen bond (q_2 value increases). Such geometry changes lead also to a H/D isotope effect on the ^{15}N chemical shift. In fact for a generic aromatic N1−H−N2 interaction at short N1−H distance, the replacement of the hydrogen by a deuteron leads to a low-frequency shift of the N1 signal. However, at long H···N2 distances, N2 resonates at higher frequency because now this distance is increased.[79]

In the case of the proton-transfer reaction from an acid AH to a base B it is well-known[69,85−88] that an increase in the AH acidity leads to a gradual transformation of the molecular hydrogen-bonded complex A−H···B to a zwitterionic complex A^-−H···B^+ via a proton-shared complex $A^{\delta-}$−H···$B^{\delta+}$. When the proton moves toward the center of the H-bond, a contraction of the A···B distance is observed. After the proton has crossed the hydrogen bond center an increase in the A···B distance results again. This transfer may be achieved by different ways, e.g., by choosing the appropriate pK_a for the acid or the pK_b for the base, by varying the temperature, by changing the solvent polarity, etc. In a symmetric HB, such as O···H···O or N···H···N,

(80) Dziembowska, T.; Ambroziak, K.; Rozwadowski, Z.; Schiff, W.; Kamienski, B. *Magn. Reson. Chem.* **2003**, *41*, 135−138.
(81) Lagier, C. M.; Apperley, D. C.; Scheler, U.; Olivieri, A. C.; Harris, R. K. *J. Chem. Soc., Faraday Trans.* **1996**, *92*, 5047−5050.
(82) Ubbelohde, A. R.; Gallagher, K. G. *Acta Crystallogr.* **1955**, *8*, 71.
(83) Legon, A. C.; Millen, D. J. *Chem. Phys. Lett.* **1988**, *147*, 484.
(84) Sokolov, N. D.; Savelev, V. A. *Chem. Phys.* **1994**, *181*, 305−317.
(85) Benedict, H.; Shenderovich, I. G.; Malkina, O. L.; Malkin, V. G.; Denisov, G. S.; Golubev, N. S.; Limbach, H. H. *J. Am. Chem. Soc.* **2000**, *122*, 1979−1988.
(86) Golubev, N. S.; Smirnov, S. N.; Gindin, V. A.; Denisov, G. S.; Benedict, H.; Limbach, H. H. *J. Am. Chem. Soc.* **1994**, *116*, 12055−12056.
(87) Golubev, N. S.; Shenderovich, I. G.; Smirnov, S. N.; Denisov, G. S.; Limbach, H. H. *Chem. Eur. J.* **1999**, *5*, 492−497.
(88) Schah-Mohammedi, P.; Shenderovich, I. G.; Detering, C.; Limbach, H. H.; Tolstoy, P. M.; Smirnov, S. N.; Denisov, G. S.; Golubev, N. S. *J. Am. Chem. Soc.* **2000**, *122*, 12878−12879.

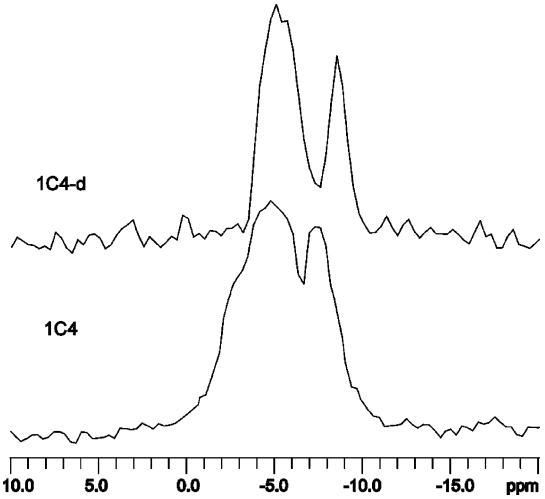

Figure 11. 27.25 MHz ^{15}N CPMAS NMR spectra of compounds **1C4** (down) and **1C4-d** (up) at 298 K, 7000 Hz spin rate.

the contraction is maximal (the heavy atoms distance q_2 is minimal) when the hydrogen lies in the center, but in the case of an asymmetric HB, such as O···H···N, the shortest HB is realized when the hydrogen lies in the "quasi-midpoint" where the O···H distance is smaller than the N···H distance.[89,90] Therefore, at the quasi-midpoint, only a small or even no geometric H/D isotope effect has been observed[79,91] and no isotope effect on the chemical shift is expected.

The ^{15}N(D) chemical shift and the H/D isotope effect on the chemical shift $^1\Delta^{15}$N(D) (defined as $\delta(^{15}\text{N}-\text{H}) - \delta(^{15}\text{N}-\text{D})$) for the adducts are reported in Table 1. According to the usual nomenclature,[92−97] superscript 1 in $^1\Delta^{15}$N(D) indicates that the ^{15}N experiencing the shift is one bond away from the deuteration site. Deuteration of **1C3** and **1C5** does not cause any shift on the ^{15}N signals. Conversely, deuteration of the **1C4** leading to **1C4-d** has a large low-frequency shift on the ^{15}N resonance at −7.2 ppm ($^1\Delta^{15}$N(D) = 1.3 ppm) and a more limited low-frequency shift for the nitrogen at −4.4 ppm ($^1\Delta^{15}$N(D) = 0.6 ppm) (Figure 11). For **1C6** the isotope effect is $^1\Delta^{15}$N(D) = 1.2 ppm from −6.5 ppm (**1C6**) to −7.8 ppm (**1C6-d**) and $^1\Delta^{15}$N(D) = 0.3 ppm from −2.5 ppm (**1C6**) to −2.8 ppm (**1C6-d**). Deuteration of **1C7** leads to a large low-frequency shift ($^1\Delta^{15}$N(D)= 1.1 ppm) of the nitrogen at −8.2 ppm, while a little smaller H/D isotope effect is observed for the nitrogen at −5.0 ppm ($^1\Delta^{15}$N(D) = 0.7 ppm). For **1C8** compound the H/D isotope effect is $^1\Delta^{15}$N(D) = 0.9 ppm from −6.6 ppm (**1C8**) to −7.5 ppm (**1C8-d**). Deuteration of **1C9** leads to a large low-frequency shift ($^1\Delta^{15}$N(D)= 1.3 ppm) of the ^{15}N signal at −8.4 ppm (**1C9**) to −9.7 ppm (**1C9-d**) similar to the shift for the signal at −4.7 ppm (**1C9**) to −5.9 ppm (**1C9-d**) ($^1\Delta^{15}$N(D) = 1.2 ppm).

Then, as expected, no shifts on deuteration are observed in the cases of **1C3** and **1C5**, characterized by weak HB. In fact it is well-known that weak hydrogen bonds do not show any H/D isotopic effect on the ^{15}N chemical shift. Conversely, a low-frequency shift is found for **1C4**, **1C6**, **1C7**, **1C8**, and **1C9** where the deuteration decreases the O−D distance and then increases the N−D distance, confirming the formation of a LBHB.

Conclusions

We have demonstrate that it is possible to correlate the isotropic ^{1}H and ^{15}N chemical shift data with the N−O distances of the atoms involved in the hydrogen bond interaction in a series of solid adducts of formula $[N(CH_2CH_2)_3N]-H-[OOC(CH_2)_nCOOH]$ (n = 1−7). The ^{1}H MAS and ^{15}N CPMAS NMR data are in agreement with the X-ray data and allow discrimination between the proton transfers for the **1C3** and **1C5** adducts, and the strong N···H−O interactions (without proton transfer) for the **1C4**, **1C7**, **1C8**, and **1C9** cocrystals. **1C6** represents an intriguing case in which one of the nitrogens of dabco is intermediate between the protonated and nonprotonated forms.

Geometry optimizations performed by density functional calculations show the localizations of the hydrogens involved in the HB interactions, in reasonable agreement with the experimental data.

The trend of the ^{15}N chemical shifts affected by the strength of the HB interaction is reproduced in the calculated data, although the theoretical treatment of hydrogen bonding is intrinsically a tough task. Although the shielding anisotropy $\Delta\sigma$ is difficult to measure, it provides a better understanding of the relationship between the magnetic properties and the molecular structure since this parameter is apparently less sensitive to the intrinsic approximations of the DFT method. In this paper we also demonstrate that the ^{1}H spectra and the isotope effect (H/D) on the ^{15}N chemical shifts represent useful tools for the characterization and classification of weak or strong HB.

One can envisage that the approach presented in this contribution, which combines solid-state NMR techniques and quantum mechanical calculations, will be especially fruitful for the investigation of hydrogen bonding in solid materials where the lack of a large crystalline order prevents the use of standard crystallographic methods.

Acknowledgment. We thank MIUR and FIRB project RBAU015MJ9 004 for financial support. We thank Dr. D. C. Apperley for recording the 300 MHz proton spectra. R.K.H. is grateful to the Leverhulme Trust for an Emeritus Fellowship.

Supporting Information Available: ^{1}H MAS NMR spectra of **1C5**−**1C9**; experimental and calculated chemical shift tensor components; ^{1}H NMR chemical shifts for **1C3**−**1C9**, and ^{13}C NMR calculated chemical shift components for **1C3**−**1C9** (pdf). This material is available free of charge via the Internet at http://pubs.acs.org.

CM049063X

(89) Steiner, T.; Saenger, W. *Acta Crystallogr., Sect. B: Struct. Sci.* **1994**, *50*, 348−357.
(90) Gilli, P.; Bertolasi, V.; Ferretti, V.; Gilli, G. *J. Am. Chem. Soc.* **1994**, *116*, 909−915.
(91) Almlöf, J. *Chem. Phys. Lett.* **1972**, *17*, 49.
(92) Gunnarson, G.; Wennerstrom, H.; Egan, W.; Forsen, S. *J. Am. Chem. Soc.* **1978**, *100*, 8264.
(93) Hansen, A. E. *Prog. Nucl. Magn. Reson. Spectrosc.* **1988**, *20*, 207.
(94) Hansen, P. E. *J. Mol. Struct.* **1994**, *321*, 79−87.
(95) Hansen, A. E.; Kawecki, R.; Krowczynski, A.; Kozerski, L. *Acta Chem. Scand.* **1990**, *44*, 836.
(96) Hansen, A. E.; Lycka, A. *Acta Chem. Scand.* **1989**, *43*, 222.
(97) Munch, M.; Hansen, A. E.; Hansen, P. E.; Bouman, T. D. *Acta Chem. Scand.* **1992**, *46*, 1065−1071.